# A new Sensorless Control for the Switched Reluctance Machine

Joanna Bekiesch and Günter Schröder
University of Siegen / Power Electronics and Electrical Drives, Siegen, Germany

***Abstract*—This paper presents a new method for determination of the rotor position of the Switched Reluctance Machine (SRM). With this it is possible to eliminate the use of the positions encoder, which is usually necessary to control the SRM. The method is based on a machine model, which includes the phase voltage equation. It can be calculated in real time. Additionally for better dynamic performance a new digital control loop is proposed. The advantages of this method are simplicity, it requires low computation time, and it gives accurate sensorless rotor position for motor operation as well as generator operation.**

## NOMENCLATURE

| | |
|---|---|
| $u$ | applied phase voltage |
| $R$ | phase winding resistance |
| $i$ | phase current |
| $di/dt$ | rate of change of the phase current in the coil of the machine |
| $\psi$ | phase flux linkage |
| $e$ | back electromotive force (back EMF) |
| $\omega$ | angular speed |
| $\theta$ | angle position of rotor |
| $L$ | absolute inductance |
| $l_{incr}$ | incremental inductance |

## I. INTRODUCTION

Switched Reluctance Motors (SRM) become more and more attractive for many industrial applications due to their simple structure, high speed, high torque and low cost, which plays a major role in industry. One of the main disadvantages of the SRM is the position encoder, which is necessary for the control of the machine.

To solve this problem, several methods for the sensorless rotor position estimation have been proposed. A classification of existing sensorless techniques was summarized in [1], [2] and [3]. Some of these methods are: flux-current detection technique [4],[5],[6],[12], model-based methods such as state observer method [7],[8],[9] , inductance model-based technique [10],[11], neural networks [12],[13] and fuzzy logic [14],[15]. Some methods are good for low and medium speed and some are good for medium and high speed. To achieve operation of the SRM in the total speed range often the combination of two methods is necessary, one for low speed and other for high speed.

This paper presents a new method to achieve improved rotor position determination for the sensorless control system at medium speed of the SRM. The method is based on a model, which includes the voltage equation. By using the measured values of terminal phase voltage, current and di/dt as inputs of the model, the rotor position determination for motor operation as well as generator operation can be done in real time.

## II. THEORETICAL ASPECT

The proposed method of the sensorless rotor position determination is based on the voltage equation describing the model of the SRM, which can be expressed as:

$$u = R \cdot i + \frac{d\psi}{dt}$$
$$u = R \cdot i + \frac{\partial \psi(i,\theta)}{\partial i} \cdot \frac{di}{dt} + \frac{\partial \psi(i,\theta)}{\partial \theta} \cdot \frac{d\theta}{dt} \quad (1)$$

This voltage equation can be transformed either under consideration of the absolute inductance $L$

$$u = R \cdot i + \frac{\partial (L(i,\theta) \cdot i)}{\partial i} \cdot \frac{di}{dt} + \omega \cdot \frac{\partial \psi(i,\theta)}{\partial \theta}$$
$$u = R \cdot i + \left[ i \cdot \frac{\partial L(i,\theta)}{\partial i} + L(i,\theta) \right] \cdot \frac{di}{dt} + i \cdot \omega \cdot \frac{\partial L(i,\theta)}{\partial \theta} \quad (2)$$

or the incremental inductance $l_{inc}$

$$u = R \cdot i + l_{incr}(i,\theta) \cdot \frac{di}{dt} + i \cdot \omega \cdot \frac{\partial L(i,\theta)}{\partial \theta} \quad (3)$$

The above equations can be obtained if we insert the $\psi(i,\theta) = L(i,\theta) \cdot i$ or the $\partial \psi(i,\theta)/\partial i = l_{incr}(i,\theta)$ terms into the $\partial \psi(i,\theta)/\partial i$ derivative in (1). From these equations it can be noticed, that the both variables $l_{incr}(i,\theta)$ and $L(i,\theta)$ are different. Their relationship can be expressed as:

$$l_{inc}(i,\theta) = i \cdot \frac{\partial L(i,\theta)}{\partial i} + L(i,\theta) \quad (4)$$

This difference is particularly noticeable in the Figures 1 and 2, which depict the graphics of the absolute and incremental inductance respectively. This absolute inductance corresponds to the slope of a straight line going through the origin and the specific point $(i; \psi(i))$ on the saturation curve (Fig.1). However the incremental inductance corresponds to the slope of the saturation curve in the point $(i; \psi(i))$ (Fig.2).

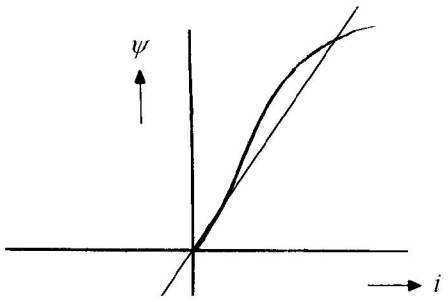


Fig. 1. Graph of the absolute inductance.

The difference between the incremental and absolute inductance has significant impact on the solution of (1). In case when the wrong inductance is chosen, the rotor position found as a solution of this equation will be not correct.

The dependence of the inductance on the frequency of the PWM has also a significant influence on the solution of the equation. By using a high frequency current change with low amplitude the inductance does not move on the saturation curve. Instead it changes in an ellipsoidal loop (Fig.3). Effective inductance corresponds here to the middle slope of the loop. In figure 3 a straight line was put through the loop, in order to clarify this. Compared with the tangent to the saturation curve in figure 2 this has a clearly smaller slope. The higher the frequency of the PWM the smaller becomes the effective inductance.

## III. Algorithm Description

To determine the rotor position one of two equations can be used (2),(3). For the equation (2) only the absolute inductance is needed, which can be determined easily. However the solution of the equation becomes very complex, since apart from the derivative $dL/d\theta$ also the derivative $dL/di$ is needed. This method is thus not practicable. A second possibility gives (3). For it both the incremental and absolute inductances are needed.

To omit unnecessary calculations and reduce the calculation time, the back EMF term given in (5) with the needed absolute inductance, can be stored in a look-up table (Fig.4).

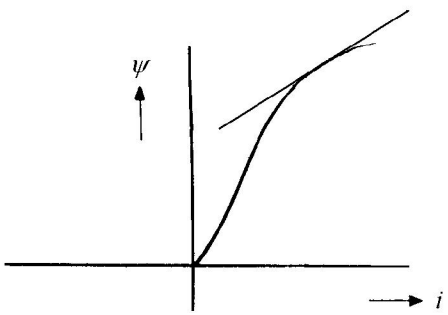


Fig. 2. Graph of the incremental inductance.

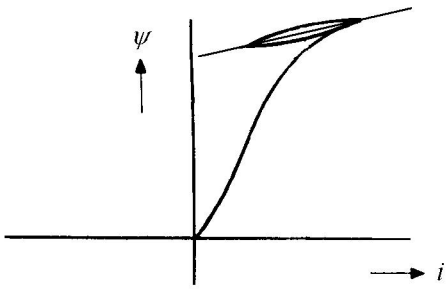


Fig. 3. Graph of the inductance depending on the frequency of PWM taking into account hysteresis.

The equation (5) represents the back EMF.

$$e(i,\theta,\omega) = i \cdot \omega \cdot \frac{\partial L(i,\theta)}{\partial \theta} \tag{5}$$

The application of look-up tables of the back EMF as well as of the incremental inductance, simplifies the calculations.

$$u = R \cdot i + l_{inc}(\theta,i)\frac{di}{dt} + e(i,\theta,\omega) \tag{6}$$

In the proposed method of the sensorless rotor position determination (6) was used. The inputs are: the current $i$ and rate of change of the phase current in the coil of the machine di/dt, which can be measured on-line, the voltage $u$ and phase winding resistance $R$, which can be assumed as constants and the incremental inductance $l_{inc}$ as well as back EMF $e$ values, which can be stored in look up tables.

To obtain the rotor position, (6) must be solved. Because incremental inductance and back EMF are used not as analytical functions of the rotor position but only in tabular form, (6) can not be solved for the rotor position.

To solve this problem (6) was transformed to the form:

$$R \cdot i + l_{incr}(i,\theta) \cdot \frac{di}{dt} + e(i,\theta,\omega) - u = 0 \tag{7}$$

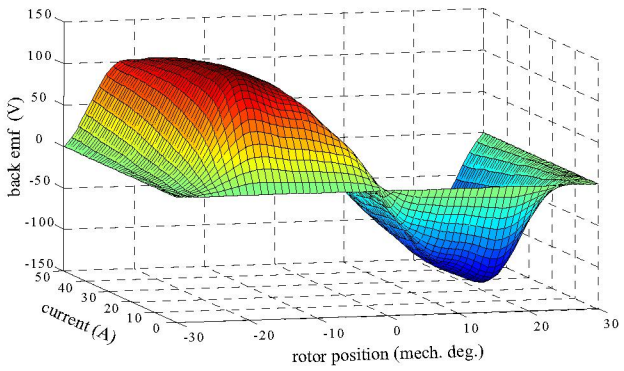


Fig. 4. Measured values of the back EMF.

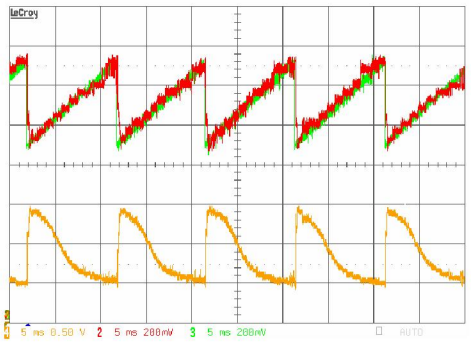

Fig. 5. Experimental result showing the rotor position of the sensor (green), sensorless rotor position (red) and di/dt (yellow) at 5A and speed at 250 rpm. Time base =5ms.

The procedure for zero-crossing searching is to pick out and put into the equation the appropriate values for incremental inductance and back EMF from the look-up tables and use them successively for all possible rotor positions. Since, dependent on the mode of operation (motor or generator operation), it is known, which phase is active in a specific rotor position range, the zero position searches can be limited to this rotor position range. This guarantees that the correct zero position is found. In addition the computing time can be reduced. Figure 5 shows the position signal of the sensor and the sensorless rotor position at 250 rpm and phase current of 5A (10% of rated current). In addition the di/dt used in the program is represented. The signal of the sensor was used to compare the sensorless position of the rotor. The control worked without sensor signal.Figure 6 presents the determined sensorless rotor position signal at a current of 10A. In the comparison to the sensorless signal determined at a current of 5A (Fig.5) this is usable however only in sub-ranges. This case is particularly noticeable at larger current. The cause for this lies in the shape of the incremental inductance, which hardly changes with large current due to saturation of the machine. Therefore the rotor position can be determined here only in a sub-range.

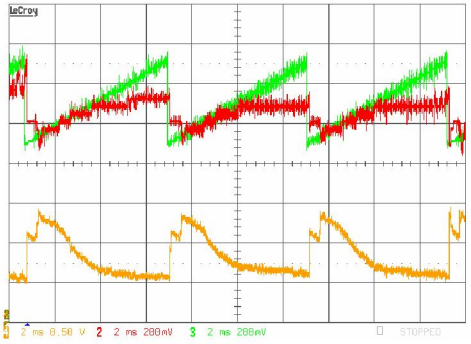

Fig. 6. Experimental result showing the rotor position of the sensor (green), sensorless rotor position (red) and di/dt (yellow) at 10A and speed at 500 rpm. Time base =2ms.

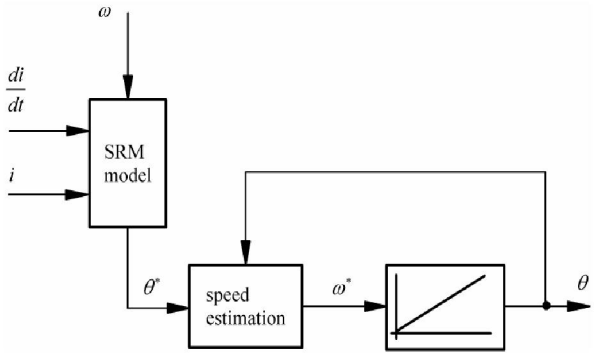


Fig. 7. Block diagram of the digital control loop.

To solve this problem a position signal must be generated from the sub-range which could be available during the whole electrical period. For this an integrator is used whose input is an estimated value for the actual speed $\omega^*$. The estimated value of speed is updated with the help of the position signal. This actualization happens naturally only within the ranges, within which the position signal of the machine model is correct. Figure 7 shows the block diagram of the proposed digital control loop.

The speed estimation block was realized with a P controller. The value of the speed was determined from the difference of the determined position $\theta^*$ from the model of the machine and the output signal of the integrator multiplied by the kp gain. In addition this estimated value was smoothed and used as input signal for the machine model.The disadvantage of the P controller is the steady state error which has negative impact on the performance of the control loop. To prevent this, compensation is proposed. The smoothed speed $\omega^{**}$ is divided by the kp of the controller and added to the output signal of the integrator. Figure 8 shows the block diagram of the proposed method, which output is the estimated position $\theta$.

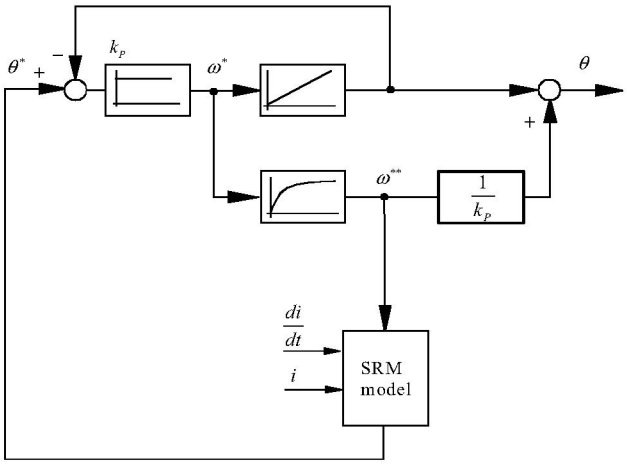


Fig. 8. Block diagram of the digital control loop with P controller and compensation of the error signal.

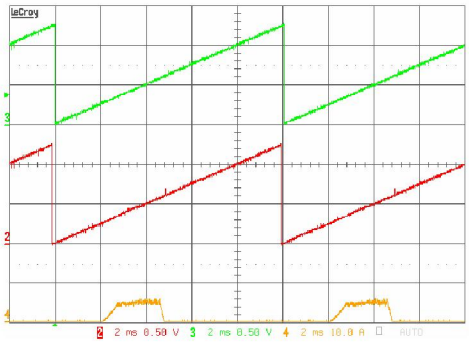

Fig. 9. Experimental result showing (top to bottom) the rotor position of the sensor, sensorless rotor position and phase current at 5A in generator operating at speed 1000 rpm. Time base =2ms.

## IV. Experimental Results

### A. *Generator operation*

Figure 9 presents the experimental results in generator operation. It shows the rotor position of the sensor, as well as the sensorless determined position. In addition the current in the active phase is represented. The measurement was accomplished at a current of 5A and a speed of 1000 rpm. It is to be noticed that the estimated rotor position agrees with the rotor position of the sensor. In a far speed range of approx. 400 rpm up to the rated speed of 1500rpm good results are obtained, which do not differ in their quality from the measurement with 1000 rpm. At larger current, up to the rated current of 50A, the result worsens only insignificantly. Below 400 rpm the position signal noticeable worsens. Figure 10 was taken at a speed of 150 rpm. There the stability limit is reached. If the speed is continuously getting lower, then the system tilts and the phases are not any longer correctly excited. The cause for this lies mainly in the shape of the back EMF, which is dependent on the speed. The smaller the speed the smaller is the back EMF and its slope.

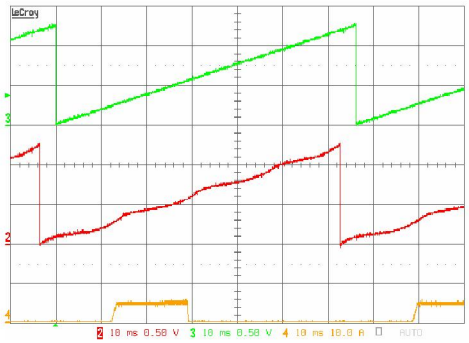

Fig. 10. Experimental result showing (top to bottom) the rotor position of the sensor, sensorless rotor position and phase current at 5A in generator operating at speed 150 rpm. Time base =10ms.

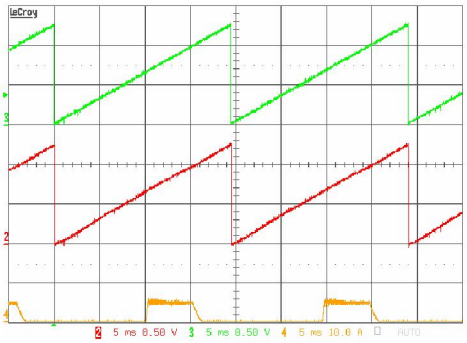

Fig. 11. Experimental result showing (top to bottom) the rotor position of the sensor, sensorless rotor position and phase current at 5A in motor operating at seed 500 rpm. Time base =5ms.

In addition the shape of di/dt, which is dependent on inductance, hardly changes with small current close to the aligned rotor position. The existence of these phenomena prevents the accurate rotor position estimation. Even the suggested digital controller loop does not improve the determination of the rotor position.

### B. *Motor operation*

First the phases in the motor operation were activated just like in the generator operation. At a small current up to approx. 7A comparable results were obtained as in the generator operation, see figure 9. Figure 11 shows the measurement result at 5A and 500 rpm. At larger current however the system becomes instable. This is caused by back EMF and di/dt, unlike to the generator operation, the values of which in sub-ranges of the rotor position are not changing (Fig.12). Thus, a precise position can not be determined.

To solve this problem, the cycle duration of the phase will be extended. Thus, the range of the back EMF and di/dt was enlarged. With this it is possible to obtain the rotor position. Figure 13 shows the experimental result at a current of 40A and a speed of 500 rpm.

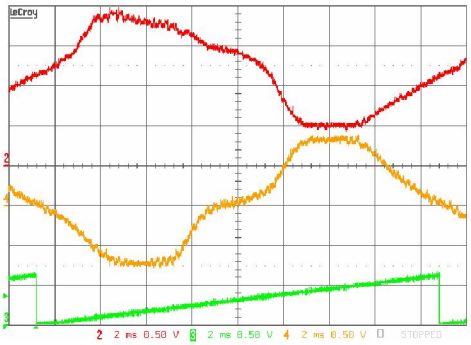

Fig. 12. Experimental result showing (top to bottom) the di/dt, back EMF and rotor position of the sensor at 16A. Time base =2ms.

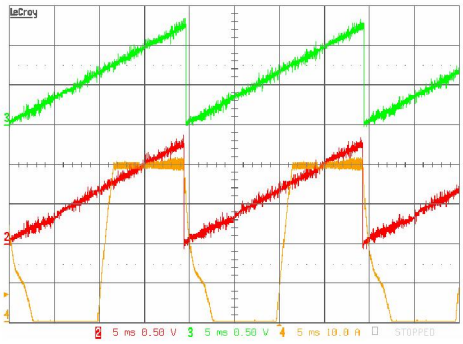

Fig. 13. Experimental result showing (top to bottom) the rotor position of the sensor, sensorless rotor position and phase current at 40A in motor operating at speed 500 rpm. Time base =5ms.

Figure 14 shows the experimental result at 15A. In the comparison of the figure 14 and figure 13 a clear shift between actual position and sensorless position is to be noticed. That is caused by the decrease of the flux, in the motor. At smaller currents, and thus smaller flux, the effect of the mutual influence is larger than with large current. At further at a constant value of speed if the current is continuously reduced the stability limit is reached with for instance 10A. The machine is not any more operated within the range of the saturation and the mutual influence becomes so large that the position signal becomes very wavy (Fig.15). To prevent this, the model of the SRM machine which has been used to obtain the sensorless rotor position, should include the mutual influence of the phases. That is the future task of our research. At 15A the motor runs in a speed range from 300 rpm to 1500 rpm sensorless. Below 300 rpm a difference arises between the sensor position and estimated position. The stability limit is reached.

To obtain high performance of the current controller a PI controller has been used with consideration of the variable time and a back EMF compensation [16],[17].

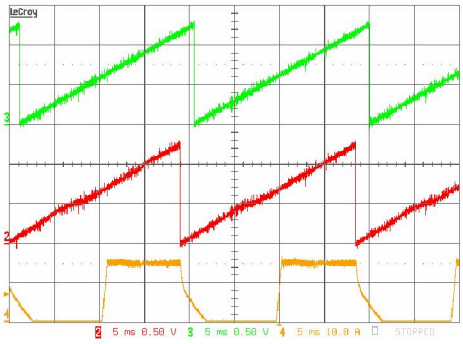

Fig. 14. Experimental result showing (top to bottom) the rotor position of the sensor, sensorless rotor position and phase current at 15A in motor operating at speed 500 rpm. Time base =5ms.

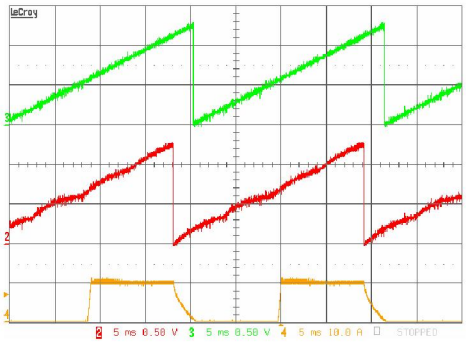

Fig. 15. Experimental result showing (top to bottom) the rotor position of the sensor, sensorless rotor position and phase current at 10A in motor operating at speed 500 rpm. Time base =5ms.

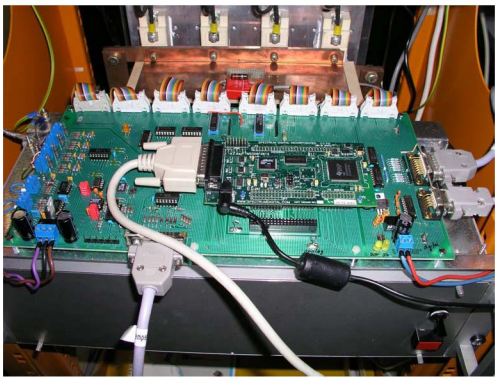

Photo 1. TMS 320F2812 DSP and Interface circuit and IGBTs (background).

TABLE I.
MOTOR RATINGS

| | |
|---|---|
| 4 phase stator/rotor poles | 8/6 |
| Power | 7,5 kW |
| DC supply voltage | 250V |
| Rated speed | 1500 rpm |
| Rated torque | 48 Nm |
| Peak phase current | 50 A |
| Max. inductance | 90 mH |
| Min. inductance | 4 mH |
| Rotor pole arc | 24 deg. |
| Stator pole arc | 20 deg. |
| Turns per pole | 70 |

## V. CONCLUSION

In this paper a method for sensorless position determination of the rotor is presented. This method improves the sensorless control of the SRM and provides an achievement of stable work of the machine at medium speed without position encoder, in motor as well as generator operation. Experimental results show good performance of the rotor position determination. This sensorless position determination of the rotor makes possible to omit the sensor and lowers thereby the costs and increases the reliability of the drive.

The proposed rotor position determination scheme is realized using a TMS320f2812 DSP (Photo 1). For the achievement of the presented experimental results in the paper a 4-ph SRM was used (Table1).

## REFERENCES


[1] T. J. E. Miller, *Electronic Control of Switched Reluctance Machines*, Oxford, UK, Newnes, 2001.

[2] R. Krishnan, *Switched Reluctance Motor Drives*, CRC Press, 2001.

[3] M. Ehsani and B. Fahimi, "Elimination of Position Sensors in Switched Reluctance Motor Drives: State of the Art and Future Trends", *IEEE Trans. On Industrial Electronics*, vol. 49, pp. 40-47, February 2002.

[4] D. Panda and V. Ramanarayanan, "Sensorless Control of Switched Reluctance Motor Drive with Self-Measured Flux-Linkage Characteristics", in *PESC 2000, Annual Power Electronics Specialists Conference,* Galway/Irland, June 18-23, 2000, pp. 1569-1574.

[5] S. K. Mondal, S. N. Saxena, S. N. Bhadra and B. P. Muni, "Evaluation of Novel Analog Based Closed-Loop Sensorless Controller for Switched Reluctance Motor Drive", in *APEC 2000, Applied Power Electronics Conference and Exposition*, New Orleans/USA, February 6-10, 2000, in CD-ROM.

[6] N. W. Fuengwarodsakul, S. E. Bauer, J. Krane Ch. P. Dick and R. W. De. Doncker, "Sensorless Direct Instantaneous Torque Control for Switched Reluctance Machines", in *EPE 2005, European Conference on Power Electronics and Applications*, Dresden/Germany, September 11-14, 2005, in CD-ROM.

[7] R. A. McCann, M S. Islam and I. Husain, "Application of a Sliding-Mode Observer for Position and Speed Estimation in Switched Reluctance Motor Drives", *IEEE Trans. On Industrial Applications*, vol. 37, pp.51-58, January/February 2001.

[8] M. S. Islam and I. Husain, "Self-tuning of Sensorless Switched Reluctance Motor Drives with Online Parameter Identification", in *IAS 2000, Industry Applications Conference*, Rome/Italy, October 8-12,2000, vol. 3, pp. 1738-1744.

[9] W. Lu and A. Keyhani, "Sensorless Control of Switched Reluctance Motors Using Sliding Mode Observers", in *IEMDC 2001, Electrical Machines and Drives Conference*, Cambridge,MA, June 17-20,2001, pp 69-72.

[10] G. Suresh, B. Fahimi, K. M. Rahman and M. Ehsani, "Inductance Based Position Encoding for Sensorless SRM Drives", in *PESC 1999, Annual Power Electronics Specialists Conference*, Charleston, July 1999, vol. 2, pp. 832-837.

[11] H. Gao, F. R. Salmasi and M. Ehsani, "Inductance Model-Based Sensorless Control of the Switched Reluctance Motor Drive at Low Speed", *IEEE Trans. On Power Electronics*, vol. 19, pp.1568-1573, November 2004.

[12] W. S. Baik, M. H. Kim, N. H. Kim, D. H. Kim, K. H. Choi, D. H.Hawang and J. S. Jang, "Improved Rotor Position Estimation for the Sensorless Control System of SRM", in *ISIE 2005. Int. Symposium on Industrial Electronics*, Dobrovnik/Kroatien, June 20-23, 2005, in CD-ROM.

[13] W. S. Baik, M. H. Kim, N. H. Kim and D. H. Kim, "Position Sensorless Control System of SRM using Neural Network", in *PESC 2004, Annual Power Electronics Specialists Conference*, Aachen/Germany, June 20-25, 2004, CD-ROM.

[14] L. O. de A. P. Henriques, L. G. B. Rolim, W. I. Suemitsu and P. J. Costa Branco, "Neuro-Fuzzy Position Online Estimation Applied in a SRM: Speed Range Experimental Results", in *PESC 2005, Annual Power Electronics Specialists Conference*, Recife/Brazil, June 12-16, 2005 in CD-Rom.

[15] A. D. Cheok and Z. Wang, "Fuzzy Logic Rotor Position Estimation Based Switched Reluctance Motor DSP Drive With Accuracy Enhancement", *IEEE Trans. On Power Electronics,* vol. 20, pp.908-921, July 2005.

[16] G. Schröder and J. Bekiesch, "Adaptive Current Control for the SRM", in *ISIE 2005, International Symposium on Industrial Electronics*, Dobrovnik/Kroatien, June 20-23, 2005, in CD-ROM.

[17] G. Schröder and J. Bekiesch, "Current Control for the Switched Reluctance Motor with Enhanced Performance", in *EPE 2005, European Conference on Power Electronics and Applications*, Dresden/Germany, September 11-14, 2005, in CD-ROM.